

WL
EMP
3-52
JN44
C.1
7-c

Interaction Notes

Note 447

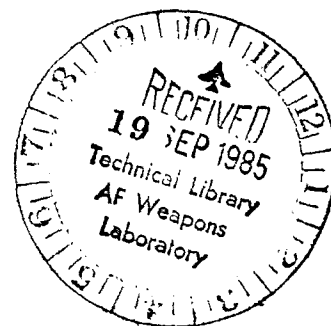
October 1984

Time Harmonic Solutions for a
Long Horizontal Wire Over the Ground
With Grazing Incidence

Kenneth C. Chen
Sandia National Laboratories, Division 7553
P.O. Box 5800
Albuquerque, New Mexico 87185

ABSTRACT

This paper presents a parametric study of the current responses on a long horizontal wire over the ground with frequencies ranging from 10 kHz to 100 MHz, earth conductivities of 10^{-1} , 10^{-2} , and 10^{-3} S/m, and wire heights of 10, 5, and 1 m. These current responses for typical wire lengths are given for a grazing incident plane wave and an incident lateral wave.



1. Introduction

The determination of the electromagnetic response of a horizontal wire over the ground has been a subject of great interest. Numerous authors [1]-[3] have treated different aspects of this problem. Carson [1] in his classic paper solved the transmission line mode for an infinite wire extended in both ends. More recently, King, Wu and Shen [3] derived the transmission line mode wave number and its characteristic impedance by taking an appropriate limit for an eccentric insulated antenna [4]. Although these important transmission line parameters, k and Z_c , are not intrinsically different from those obtained by Carson, King et al did derive them rigorously and express these quantities in terms of tabulated functions, and thus facilitate the computation. Furthermore, they observed that in order for a transmission line mode to be a good approximation to the total solution of Maxwell's equations, the following two conditions must be met:

$$|k_4|^2 \gg |k_0|^2 \quad (1)$$

and

$$|k_0 d| \ll 1 \quad (2)$$

where k_0 and k_4 are the wave numbers for the air and ground, respectively and d is the height above the ground. From (1), they [3] pointed out that the theory is applicable to high frequencies when the ground behaves more like a dielectric than a good conductor, which is more general than Carson has assumed.

The starting point of this paper is King et al's rigorous theory. It is important to point out that that theory is valid

for the transmission line mode for all values of $|k_0 d|$. This is because the transmission line mode satisfies a transverse Laplace equation in the air (where the wave number is k_0). To obtain a complete solution to the Maxwell's equations, one has to find all other discrete modes and the branch cut contribution. Although a complete solution is not given here, it is worthwhile to show how to obtain the transmission line mode for all $|k_0 d|$. One can argue that under the excitation of an incident wave, the transmission line mode is likely to dominate the total solution. However, when the excitation is localized, the solution near the source is likely to be mostly transmission line mode, and the solution far away from the source is likely to be dominated by the branch cut contribution. A complete solution of the overhead wire problem requires Wiener-Hopf solutions of an integral equation with the interface kernel and the various excitation conditions, which is not the purpose of this paper. Our purpose here is to use the transmission line solution to solve the following important problem: the time harmonic solutions for a finite horizontal wire over the ground with grazing incidence. During the completion of this paper, an interesting paper by King and Shen [5] appeared. Although general formulas for transmission line theory given in this paper are similar to theirs, applications of these formulas are completely different. King et al's principal objective is to obtain the current and the fields scattered by a short thin wire over a material half-space. Our objective here is to determine the

induced current on a long wire over the ground under grazing incidence.

Previous results on a horizontal wire under a grazing incidence [6][7] are limited to wires with an infinite length extended in both directions. The new findings reported in this paper are: one, the numerical results of wire currents for both infinite and finite wires with grazing incident plane waves and incident lateral waves; two, the wire length required for a finite wire to attain a maximum grazing current; three, the current distribution on a finite wire with various loads under a grazing incidence plane wave and an incident lateral wave; and finally, the transition of current responses from a finite wire to an infinite wire. Although this study is based on King et al's [3] theory, it is important to point out that, since the transmission line wave number is very close to k_0 , it is necessary to calculate the transmission line parameters to much greater accuracy than that provided by the small argument formula. Thus, the numerical determination of these parameters for all ranges is important. Furthermore, under conditions (1) and (2), it is possible to have $|k_4| d \gg 1$ such that the large argument approximation becomes relevant to the analysis.

In summary, Section 2 discusses the transmission line theory for the wire over the ground with special emphasis on the different limiting cases for the transmission line parameters. Section 3 gives an elementary account of how to determine the transmission line current and voltage from the Green's function of transmission

line equations and discusses their applications to calculating the grazing currents on the wires. The most significant contribution of this paper is the collection of the numerical results, which show the current responses of wires over the ground under grazing incidence. They are also given in Section 3.

2. The Wave Number and Characteristic Impedance for the Transmission Line Mode.

Formulas [3] for the wave number and characteristic impedance are given as ($e^{-i\omega t}$ time dependence)

$$k = (-ZY)^{1/2} \quad (3)$$

and

$$Z_c = (Z/Y)^{1/2} \quad (4)$$

with

$$Y = -i\omega C,$$

C = wire capacitance to the ground per meter

$$= \frac{2\pi\epsilon_0}{\Omega}, \quad \Omega = \text{arccosh}(d/a), \quad a = \text{wire radius}$$

and d = wire height,

and

$$Z = -i\omega L,$$

$$L = L_1 + L_2$$

$$L_1 = \text{wire inductance in air per meter} = \frac{\mu\Omega}{2\pi}$$

$L_2 =$ inductance in the ground per meter

$$= \frac{\mu\Delta}{2\pi}$$

Here Δ is given by

$$\Delta = 2 \left\{ \frac{1}{A^2} - \frac{K_1(A)}{A} + \frac{i\pi I_1(A)}{2A} - \frac{i\pi}{2A} \left[E_1(iA) - \frac{2i}{\pi} \right] \right\} \quad (5)$$

with

$$\frac{i\pi}{2A} \left[E_1(iA) - \frac{2i}{\pi} \right] = i \left[\frac{A}{3} + \frac{A^3}{45} + \frac{A^5}{1575} + \frac{A^7}{99225} + \dots \right] \quad (6)$$

I_1 and K_1 are the modified Bessel functions of the first and second kind, respectively, and the first order. E_1 is the Weber function of the first order, and finally A is given by

$$A = 2k_4 d, \quad k_4 = \sqrt{\omega\mu(i\sigma_4 + \omega\epsilon_0\epsilon_r4)} \quad (7)$$

Equation (5) is given explicitly by King et al. However, since I_1 and E_1 both diverge for large values of A , it is necessary to obtain an alternate formula for Δ . Appendix A shows for $|k_4 d| \gg 1$,

$$\Delta \sim \frac{2}{A^2} + \frac{2i}{A} \left\{ 1 + \frac{1}{(iA)^2} - \frac{3}{(iA)^4} + \frac{45}{(iA)^6} - \frac{1575}{(iA)^8} + \dots \right\} - \frac{4K_1(A)}{A} \quad (8)$$

Notice (8) differs from (A20) given in Reference 3 in the numerical coefficient of the last term.

The leading term in the expansion for (5) is

$$\Delta \sim \frac{i}{k_4 d},$$

and its corresponding impedance is

$$Z_2 = -i\omega L_2 = \frac{-i\mu\omega}{2\pi} \Delta \sim \frac{1}{2\pi d} \left(\frac{\omega\mu}{2\sigma_4} \right)^{1/2} (1-i) \quad (9)$$

for $\sigma_4 \gg \omega\epsilon_0\epsilon_r4$

It is interesting to note that this term is the same as would be obtained in a coax with the outer coaxial conductor of radius d [4]. This fact has never been noted before. The ratio of the wave number to the free space wave number can now be calculated as

$$\zeta_L = \frac{k}{k_0} = \left(1 + \frac{\Delta}{\Omega}\right)^{1/2} \quad (10)$$

The characteristic impedance is

$$Z_c = \frac{\Omega}{2\pi} \left(\frac{\mu}{\epsilon}\right)^{1/2} \zeta_L = Z_0 \zeta_L \quad (11)$$

where Z_0 is the characteristic impedance for a wire over a perfectly conducting ground plane with the same configuration.

In order to determine the ranges of validity for Equations (5) and (8), we plotted (5) for small values of A and (8) for large values of A . Furthermore, we compared these values to those calculated from the numerical integration of Δ given in (A-1), that is

$$\Delta = \Delta(A,0) = \frac{2}{A^2} + 2i \int_0^1 (1-x^2)^{1/2} \exp(-Ax) dx - \frac{2K_1(A)}{A} \quad (12)$$

In Figure 1, the value of Δ calculated from these three equations are compared for real A , which is relevant for a dielectric half space, such as lake water. In Figure 2, the values of Δ calculated from these three equations are compared for $\text{Arg}(A) = 45^\circ$, which is relevant for a conducting ground. It is interesting to note that for $|A| < 3.5$ Equation (5) gives a fairly accurate result. On the

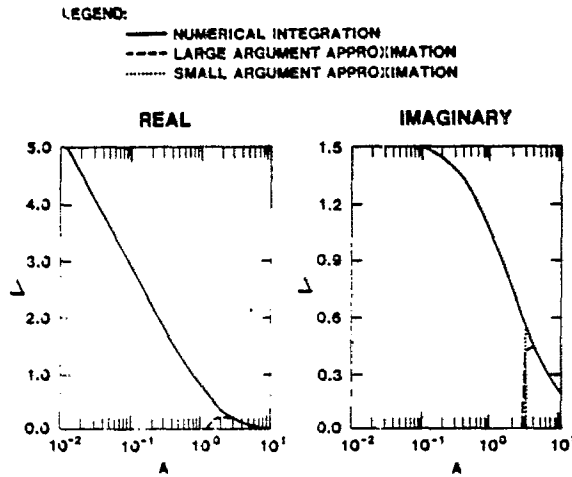


Figure 1. Comparison of Three Different Ways of Calculating Δ for Real A . The small argument formula for the real part of Δ coincides with the integration scheme. This is relevant for a dielectric half space.

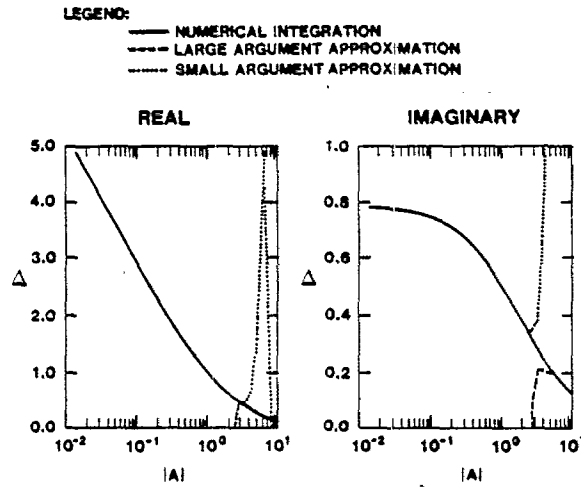


Figure 2. Comparison of Three Different Ways of Calculating W for $A = |A| e^{i4/\pi}$. This is relevant for a conducting half space.

other hand, for $|A| > 3.5$ Equation (8) is quite accurate numerically. When $|A| > 10$, the leading term $i\frac{2}{A}$ gives better than 10 percent accuracy. For $|A| < 0.3$, a small argument approximation to Equation (5) which is

$$\Delta_0 = -\ln\left(\frac{A}{2}\right) - \gamma + \frac{1}{2} + i\left(\frac{\pi}{2} - \frac{2A}{3}\right) \quad (13)$$

gives better than 10 percent accuracy. Notice when using (6) for power lines at a frequency of 60Hz, one needs to calculate the Bessel functions to 12 figures to give two figures accuracy in Δ . In this case, (13) is more accurate and convenient to use.

3. Time Harmonic Solutions for Grazing Incidence

Induced currents on a thin infinite wire near the ground have been calculated in the past [6][7]. The transmission line theory developed is useful for describing the current induced on a finite length thin wire near the earth with grazing incidence (Figure 3). Advantages of this simple transmission line theory include (1) only simple and standard transmission line theory is required, so that parametric studies can be made easily; (2) it is possible to determine the minimum wire length when the maximum grazing current occurs; (3) the effects of wire termination at both ends can be incorporated; and (4) the difference between finite and infinite wire responses can be determined. Let us define K_V and K_I as the Green's functions for the following transmission line equations:

$$\begin{aligned} \frac{\partial K_V}{\partial z} + ZK_I &= \delta(z - z') \\ \frac{\partial K_I}{\partial z} + YK_V &= 0 \end{aligned} \quad (14)$$

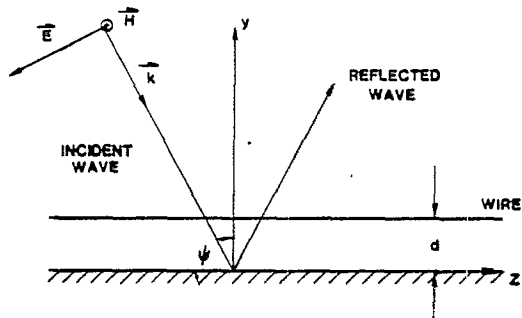


Figure 3. Configuration of a Wire Over the Ground Excited by an H-Polarized Incident Wave

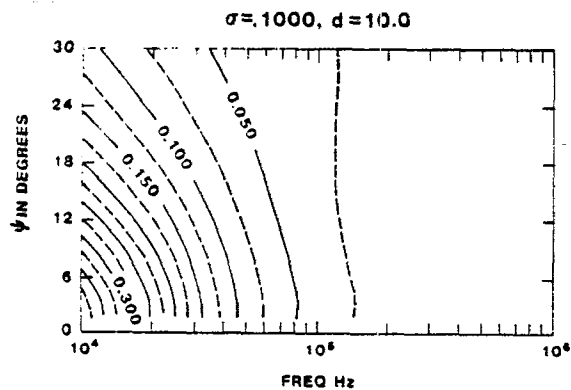


Figure 4. Induced Current in Amps for an Infinite Wire Over the Ground for a CW With Frequency and Grazing Angle Shown as Parameters. $a = 1.75$ cm, d in meters. The incident electric field is 1 V/m.

for,

$$-h \leq z \leq h,$$

and the boundary conditions,

$$\frac{K_V(-h)}{K_I(-h)} = Z_1 \quad \text{and} \quad \frac{K_V(h)}{K_I(h)} = Z_2$$

Then

$$K_I(z, z') = \begin{cases} \frac{1}{2Z_c} \left[\frac{1 - P_1 e^{i2k(h+z')}}{1 - P_1 P_2 e^{i4kh}} \right] \left[e^{ik(z-z')} - P_2 e^{i2k(h-z')} - ik(z-z') \right] & \text{for } z > z' \\ \frac{1}{2Z_c} \left[\frac{1 - P_1 e^{i2k(h-z')}}{1 - P_1 P_2 e^{i4kh}} \right] \left[e^{ik(z'-z)} - P_1 e^{i2k(h+z')} + ik(z-z') \right] & \text{for } z < z' \end{cases} \quad (15)$$

$$\text{where } P_{1,2} = \frac{Z_{1,2} - Z_c}{Z_{1,2} + Z_c},$$

and Z_c and k are given in Equations (3) and (4).

The electric field exciting the wire current is given by

$$E_z(z) = E_0 \sin \psi (1 - R_h) e^{ik_0 z \cos \psi} \quad (16)$$

where R_h is the reflection coefficient for the magnetic field parallel to the interface, ie

$$R_h = \frac{N^2 \sin \psi - (N^2 - \cos^2 \psi)^{1/2}}{N^2 \sin \psi + (N^2 - \cos^2 \psi)^{1/2}} \quad (17)$$

$$N = \frac{k_4}{k_0}$$

and E_0 is the incident electric field.

The discussion is limited to the H-polarized case here, because the total horizontal electric field available for excitation is about a factor of 5 smaller for the E-polarized case than that for

the H-polarized case. One can easily see this by comparing $1-R_H$ to $1-R_E$.

The induced wire current is given by

$$\begin{aligned}
 I(z) &= \int_{-h}^h K_I(z, z') E_z(z') dz' \\
 &= \frac{E_0 \sin \psi (1 - R_h)}{2Z_c (1 - P_1 P_2 e^{i4kh})} \left[\frac{e^{ik_0 z \cos \psi} - e^{ik(h+z) - ik_0 h \cos \psi}}{i(k_0 \cos \psi - k)} \right. \\
 &+ \frac{e^{ik(h-z) + ik_0 h \cos \psi} - e^{ik_0 z \cos \psi}}{i(k_0 \cos \psi + k)} \\
 &+ P_1 \frac{e^{ik(h+z) - ik_0 h \cos \psi} - e^{ik(3h+z) + ik_0 h \cos \psi}}{i(k_0 \cos \psi + k)} \\
 &+ P_2 \frac{e^{ik(h-z) - ik_0 h \cos \psi} - e^{ik(3h-z) - ik_0 h \cos \psi}}{i(k_0 \cos \psi - k)} \\
 &+ P_1 P_2 \left\{ \frac{e^{ik(3h+z) + ik_0 h \cos \psi} - e^{i4kh + ik_0 z \cos \psi}}{i(k_0 \cos \psi - k)} \right. \\
 &\left. - \frac{e^{ik(3h-z) + ik_0 h \cos \psi} - e^{i4kh - ik_0 z \cos \psi}}{i(k_0 \cos \psi + k)} \right\} \quad (18)
 \end{aligned}$$

Equation (18) differs from Equation (24) of Reference [5] in that it includes arbitrary terminating impedances.

In principle, Equation (18) can be plotted to give any physical parameters of interest. In this paper Equation (18) is examined numerically in great detail. First, let us note that by letting $h \rightarrow \infty$, we obtain the induced current for an infinite wire.

$$I_{\infty} = \frac{E_0 \sin \psi (1 - R_h)}{2Z_c} \left[\frac{e^{ik_0 z \cos \psi}}{i(k_0 \cos \psi - k)} - \frac{e^{ik_0 z \cos \psi}}{i(k_0 \cos \psi + k)} \right] \quad (19)$$

In Figures 4 through 12 are shown $|I_{\infty}|$ for $\psi < 30^\circ$; $10^4 < f < 10^7$ Hz; and $\sigma_4 = 10^{-1}, 10^{-2}, 10^{-3}$ S/m, $\epsilon_{r4} = 20$. The wire parameters chosen are the wire radius $a = 1.75$ cm and wire heights: $d = 10, 5,$ and 1 m.

It is interesting to note that for $d = 10$ m and $f = 500$ kHz. Figure 7 shows a maximum current of about 0.2 Amp for 1 V/m of incident wave. This corresponds to a case given in Figure 3 of [7] for the infinite wire where $d = 10$ m and the wire radius = 1 cm. In their graph the current is normalized by k_0 and given for 1 Amp/m of incident magnetic field. The agreement of their maximum current and our result on this value is very good. A close examination of these figures reveals three numerical trends: (1) The induced wire current is not proportional to the height. It decreases by less than a factor of 2 as the wire height is reduced by a decade. (2) As the frequency increases, the induced current decreases by about a factor of 2 per decade increase in frequency. (3) In the low frequency conductivity dominating situation, the induced current reduces by about a factor of 2 per decade increase in conductivity.

In order to determine how the finite wires respond differently from the infinite wires, let us graph Equation (18) for a typical length defined by

$$h = \frac{\pi}{\text{Re}(k) - k_0} \quad (20)$$

The significance of this length is that it gives the typical length when the grazing would result in a maximum current response.

Figures 13 through 19 give the magnitude of wire current for a grazing angle, matched load, and for $f = 10$ kHz, 30 kHz, 100 kHz, 300 kHz, 1 MHz, 3 MHz, 10 MHz, 30 MHz, and 100 MHz,

$$\sigma = 10^{-2} \text{ S/m}$$

$d = 10$ and the wire radius $a = 1.75$ cm. Notice the maximum grazing current for the finite wire with h given by (18) can be 50 percent higher in magnitude than the infinite wire.

It is important to interpret Equation (18) physically. Basically, a finite wire subject to an incident plane wave generates three waves with wave numbers k , $k - k_0 \cos \psi$, and $k + k_0 \cos \psi$, which causes the ripples, Figures 13 - 19, near the right hand termination. We expect the higher order modes can introduce similar ripples.

Let us define "grazing length" as the wire length required for the wire current to reach a maximum current. Table 1 shows the grazing lengths for $\sigma = 10^{-1}$ S/m and $d = 10, 5, \text{ and } 1$ m. Notice the grazing lengths are proportional to the wire heights at high frequencies. Grazing lengths for other conductivities are found to decrease by about a factor of 2 as the conductivity decreases by a decade.

Let us summarize the difference between the current responses of an infinite wire and that of a finite wire. First, when the wire is shorter than that shown in Table 1 for the particular frequency of excitation, current responses for the shorter wire, except for the ripples, are the same as shown on the left end of

the truncated long wire of equal length. Second, as the wire approaches the grazing length, the wire current becomes somewhat higher than that of the infinite wire. Then, as the wire length increases further, it gradually oscillates, and finally converges to the value for the infinite wire case.

TABLE I

Grazing Lengths for Three Different Wire Heights $d = 10, 5, \text{ and } 1 \text{ m}$, for Frequencies From 10 kHz up to 100 MHz, and a Ground Conductivity of $\sigma = 10^{-1} \text{ S/m}$

f	10 k	30 k	100 k	300 k	1 M	3 M
Grazing Length (m)	100 k	60 k	30 k	12 k	6 k	3 k

(a) $d = 10 \text{ m}$

f	10 k	30 k	100 k	300 k	1 M	3 M	10 M
Grazing Length (m)	80 k	40 k	15 k	8 k	4 k	2 k	1 k

(b) $d = 5 \text{ m}$

f	10 k	30 k	100 k	300 k	1 M	3 M	10 M	30 M
Grazing Length (m)	50 k	20 k	6 k	2 k	1 k	400	200	100

The cases when both ends are open circuited are studied numerically. As the incident wave comes in from the left, typical graphs (Figures 20 through 23) show reflection from the right and the beating associated with the incident current and reflected current. The current waveform for the open circuited case can be deduced from that for the matched load by observing the standing wave of the transmission line having wave number k .

The above calculations assumed an incident plane wave with an angle of incidence, ψ . They are relevant calculations, since for this frequency range the time harmonic signals are radiated by dipoles on the earth surface and bounced back to the ground by the ionosphere. However, it is important to point out that when the angle of incidence is less than $\arcsin |k_0/k_4|$, the plane wave incidence on a horizontal wire is an ill-posed problem. Because of the ground loss, the electric field is tilted at an angle $\chi = \arcsin |k_0/k_4|$. Therefore, the results shown in Figures 4 through 12 for $\psi < \chi$ are not valid, since the ratio of the total horizontal electric field to the total vertical electric field is given by $\sin \chi = |k_0/k_4|$. To put it another way, when the incident wave with an angle of incidence ψ as defined in Equation (16) is less than χ the horizontal electric field component is dominated by the horizontal electric field component of a lateral wave whenever such a wave exists. Under such a circumstance, the induced wire current can be calculated by assuming a horizontal electric field as follows:

$$E_z(z) = 2E_0 \frac{k_0}{k_4} e^{ik_0 z \cos \psi} \quad (21)$$

$I(z)$ is given as Equation (18) with $E_0 \sin \psi(1 - R_h)$ replaced by Equation (21) and $\psi = 0$. As a result, Equation (18) can be simplified, when $E_0 = 1$ V/m, to

$$\text{Max } \{|I(z)|\} \sim \frac{2k_0}{k_4} \frac{1}{(k - k_0)} \quad (22)$$

for $E_0 = 1$ V/m.

Figures 24 through 35 show the current responses for a horizontal wire with wire length given by (20) for the following parameters: $\sigma = 10^{-1}$, 10^{-2} , and 10^{-3} S/m, $d = 10$ m, and $f = 30$ kHz, 100 kHz, 300 kHz, and 1 MHz.

Equation (20) is found to be a slowly varying function of f , σ , and d . Let $d = 10$ m, $f = 300$ kHz and above, $\text{Max } |I(z)|$ tends to a constant, which can be shown easily from the large argument formula for k or Δ . That constant value is 0.09 Amp for $\sigma = 10^{-3}$ S/m. At lower frequencies, the maximum current becomes slightly higher for $\sigma = 10^{-2}$ S/m at 100 kHz and 0.19 Amp for $\sigma = 10^{-2}$ S/m at 30 kHz; it becomes 0.25 Amp for $\sigma = 10^{-3}$ S/m at 100 kHz, and 0.35 Amp for $\sigma = 10^{-3}$ S/m at 30 kHz.

The grazing length and the dependence of the maximum wire current on d are about the same as that for an incident plane wave.

Finally, to determine whether the lateral wave is excited on the ground surface, it is necessary to know the source characteristics, which includes the location of the source with respect to the receiving horizontal wire and the interface. A complete current response characterization with these parameters

can be obtained by using the famous lateral wave field expression [8] as the incident field. Furthermore, to obtain a realistic current response for a long wire over the earth due to a dipole source, it is necessary to use the field expression near the earth first obtained by Van der Pol and Bremmer [9]. Finally, the induced voltages on the vertical elements must be included. However, this equivalent Thevenin voltage is independent of angle of incidence and the ground conductivity and is proportional to wire height for grazing incidence. They can be easily included.

4. Conclusions

A simple procedure has been described for calculating the important transmission line parameter, k and Z_c , for all frequencies. This simple procedure has been applied to a parametric study of the long horizontal wire responses with grazing plane waves and a lateral wave.

Acknowledgment

The author would like to thank Mr. Kenneth M. Damrau for performing the numerical computations.

References

1. J. R. Carson, "Wave Propagation in Overhead Wires With Ground Return," Bell System Tech Journal, Vol. 5, pp. 539-554, 1926.
2. J. R. Wait, "Theory of Wave Propagation Along a Thin Wire Parallel to an Interface," Radio Science, Vol. 7, pp. 675-679, 1972.

3. R. W. P. King, T. T. Wu, and L. C. Shen, "The Horizontal-Wire Antenna Over a Conducting or Dielectric Half-Space: Current and Admittance," *Radio Science*, Vol. 9, pp. 701-709, July 1974.
4. R. W. P. King, and G. S. Smith, Antennas in Matter, MIT Press, Cambridge, MA, p. 11, 1981.
5. R. W. P. King and L. C. Shen, "Scattering by Wires Near a Material Half Space," *IEEE Trans. AP-30*, No. 6., 1983.
6. D. C. Chang and R. G. Olsen, "Excitation of an Infinite Antenna Above a Dissipative Earth," *Radio Science*, Vol. 10, no. 8, 9, pp. 823-831, August-September 1975.
7. R. G. Olsen and D. C. Chang, "Current Induced by a Plane Wave on a Thin Infinite Wire Near the Earth," *IEEE Trans. Antennas Propagat.*, Vol. AP-22, No. 4, pp. 586-589, July 1974.
8. P. C. Clemmow, "The Plane Wave Spectrum Representation of Electromagnetic Fields," New York: Pergamon, 1966, p. 109.
9. N. A. Logan and K. S. Yee, "A Mathematical Model for Diffraction by Convex Surfaces, in *Electromagnetic Waves*," University of Wisconsin Press, 1962.
10. J. R. Wait, "Comments on the Horizontal Wire Antenna," *Radio Science*, Vol. 9, p. 1165, 1974.
11. I. S. Gradshteyn and I. M. Ryzhik, *Tables of Integrals, Series, and Product*, New York: Academic, 1980.
12. M. Abramowitz and I. A. Stegun, "Handbook of Mathematical Functions," AMS 55, National Bureau of Standards, 1972.

APPENDIX A

Derivation of Asymptotic Formulas for
 $|k_4|d \gg 1$

King et al, derived the transmission line wave number and the axial electric field at the interface in terms of the following important integral:

$$\Delta(A,B) = 2 \left\{ \int_0^1 [x + i(1-x^2)^{1/2}] e^{-Ax} \cos Bxdx \right. \\ \left. + \int_1^\infty [x - (x^2 - 1)^{1/2}] e^{-Ax} \cos Bxdx \right\} \quad (A-1)$$

where

$$A = 2k_4d, \quad B = k_4L$$

Similar integrals were obtained by others. [1]-[9] Equation (A-1) is evaluated for real k_4 in [3] and then extended to complex k_4 by an analytical continuation argument.

It is instructive to show the same answer emerges when (A-1) is evaluated for complex k_4 . Let us rewrite (A-1) as follows:

$$\Delta(A,B) = 2 \int_0^\infty xe^{-Ax} \cos Bxdx \\ + i \left[\int_0^1 (1-x^2)^{1/2} e^{-(iB-A)x} dx + \int_0^1 (1-x^2)^{1/2} e^{-(iB-A)x} dx \right]$$

$$- \left[\int_1^{\infty} (x^2 - 1)^{1/2} e^{-(A - iB)x} dx + \int_1^{\infty} (x^2 - 1)^{1/2} e^{-(A + iB)x} dx \right] \quad (A-2)$$

The integrals in (A-2) can be identified, [10] and (A-2) reduces to

$$\begin{aligned} \Delta(A, B) &= \frac{2(A^2 - B^2)}{(A^2 + B^2)^2} + \frac{i\pi/2}{(-A + iB)} \left[I_1(iB - A) + L_1(iB - A) \right] \\ &+ \frac{i\pi/2}{(-A - iB)} \left[I_1(-iB - A) + L_1(-iB - A) \right] \\ &- \frac{K_1(A - iB)}{(A - iB)} - \frac{K_1(A + iB)}{(A + iB)} \end{aligned}$$

Here L_1 is a modified Struve function [11]

When $B = 0$,

$$\Delta(A, 0) = \frac{2}{A^2} - \frac{i\pi}{A} \left[I_1(-A) + L_1(-A) \right] - \frac{2K_1(A)}{A}$$

Here, $I_1(A)$ is an odd function and $L_1(A)$ is an even function.

Therefore,

$$\Delta(A, 0) = \frac{2}{A^2} + \frac{i\pi}{A} \left[I_1(A) - L_1(A) \right] - \frac{2K_1(A)}{A} \quad (A-3)$$

Next, on using the identity [12]

$$L_1(A) = -H_1(iA) = E_1(iA) - \frac{2}{\pi}$$

(A-3) is reduced to

$$\Delta(A,0) = \frac{2}{A^2} + \frac{i\pi}{A} \left[I_1(A) - E_1(iA) + \frac{2}{\pi} \right] - \frac{2K_1(A)}{A} \quad (A-4)$$

Equation (A-4) is in agreement with Equation (A-14) of King et al.

In order to derive Δ for $|k_4|d \gg 1$, we invoke the following formulas:

$$L_1(A) = -H_1(iA) \sim -Y_1(iA) - \frac{2}{\pi} \left[1 + \frac{1}{(iA)^2} - \frac{1^2 \cdot 3}{(iA)^4} + \frac{1^2 \cdot 3^2 \cdot 5}{(iA)^6} - \frac{1^2 \cdot 3^2 \cdot 5^2 \cdot 7}{(iA)^8} + \dots \right], |Arg(iA)| < \pi \quad (A-5)$$

and

$$I_1(A) = -iJ_1(iA) \quad (A-6)$$

Equations (A-5), (A-6) and (A-3) give

$$\begin{aligned} \Delta(A,0) &= \frac{2}{A^2} + \frac{\pi}{A} [J_1(iA) + iY_1(iA)] \\ &+ \frac{i2}{A} \left[1 + \frac{1}{(iA)^2} - \frac{1^2 \cdot 3}{(iA)^4} + \frac{1^2 \cdot 3^2 \cdot 5}{(iA)^6} - \frac{1^2 \cdot 3^2 \cdot 5^2 \cdot 7}{(iA)^8} + \dots \right] \\ &- \frac{2K_1(A)}{A} \\ &= \frac{2}{A^2} - \frac{4K_1(A)}{A} + \frac{i2}{A} \left[1 + \frac{1}{(iA)^2} - \frac{1^2 \cdot 3}{(iA)^4} + \frac{1^2 \cdot 3^2 \cdot 5}{(iA)^6} - \frac{1^2 \cdot 3^2 \cdot 5^2 \cdot 7}{(iA)^8} + \dots \right] \end{aligned} \quad (A-7)$$

is is the equation given in (6) except $\Delta(A,0)$ is denoted as Δ there.

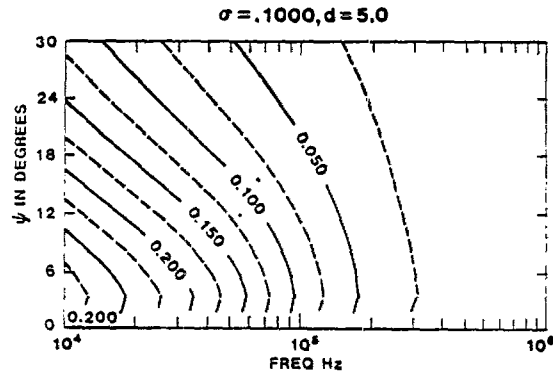


Figure 5. Induced Current in Amps for an Infinite Wire Over the Ground for a CW With Frequency and Grazing Angle Shown as Parameters. $a = 1.75$ cm, d in meters. The incident electric field is 1 V/m.

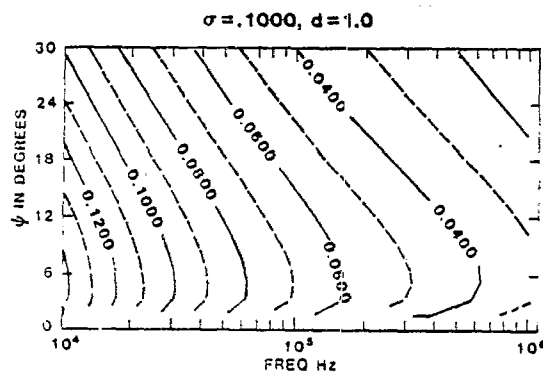


Figure 6. Induced Current in Amps for an Infinite Wire Over the Ground for a CW With Frequency and Grazing Angle Shown as Parameters. $a = 1.75$ cm, d in meters. The incident electric field is 1 V/m.

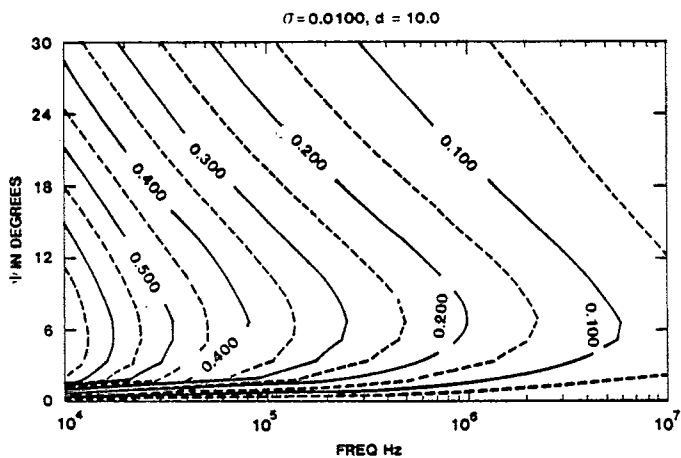


Figure 7. Induced Current in Amps for an Infinite Wire Over the Ground for a CW With Frequency and Grazing Angle Shown as Parameters. $a = 1.75$ cm, d in meters. The incident electric field is 1 V/m.

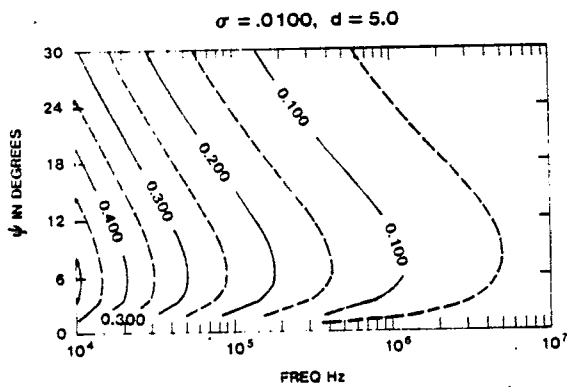


Figure 8. Induced Current in Amps for an Infinite Wire Over the Ground for a CW With Frequency and Grazing Angle Shown as Parameters. $a = 1.75$ cm, d in meters. The incident electric field is 1 V/m.

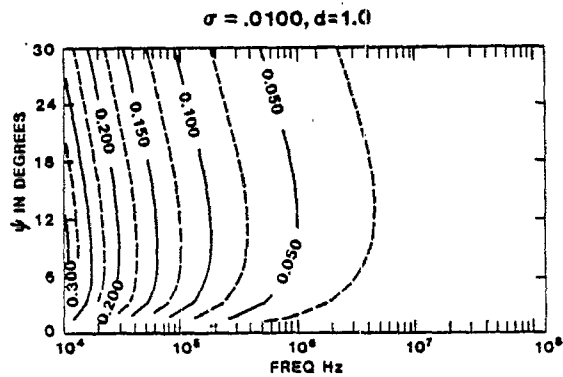


Figure 9. Induced Current in Amps for an Infinite Wire Over the Ground for a CW With Frequency and Grazing Angle Shown as Parameters. $a = 1.75$ cm, d in meters. The incident electric field is 1 V/m.

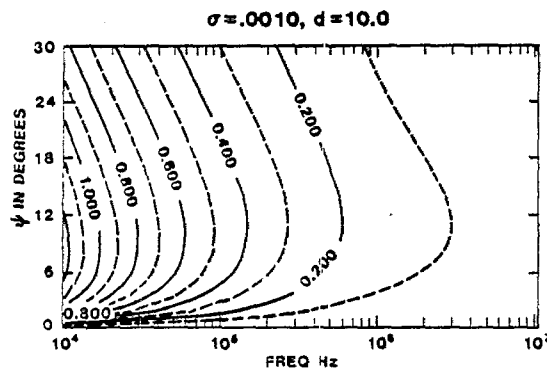


Figure 10. Induced Current in Amps for an Infinite Wire Over the Ground for a CW With Frequency and Grazing Angle Shown as Parameters. $a = 1.75$ cm, d in meters. The incident electric field is 1 V/m.

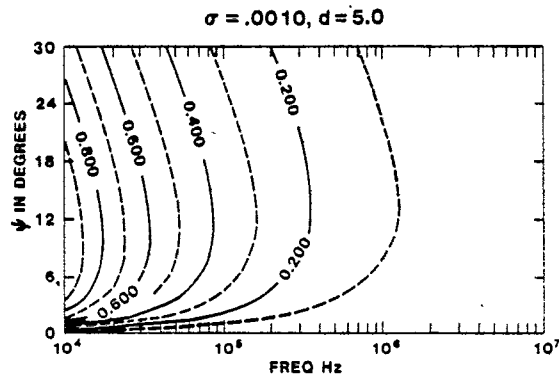


Figure 11. Induced Current in Amps for an Infinite Wire Over the Ground for a CW With Frequency and Grazing Angle Shown as Parameters. $a = 1.75$ cm, d in meters. The incident electric field is 1 V/m.

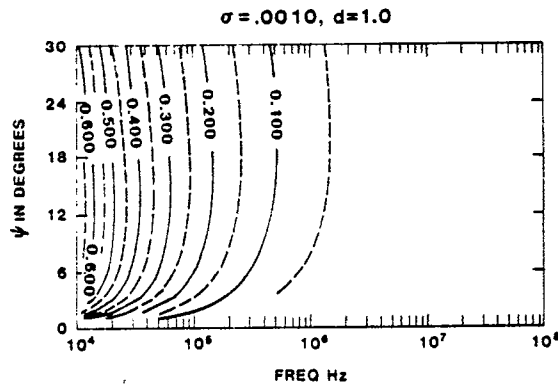


Figure 12. Induced Current in Amps for an Infinite Wire Over the Ground for a CW With Frequency and Grazing Angle Shown as Parameters. $a = 1.75$ cm, d in meters. The incident electric field is 1 V/m.

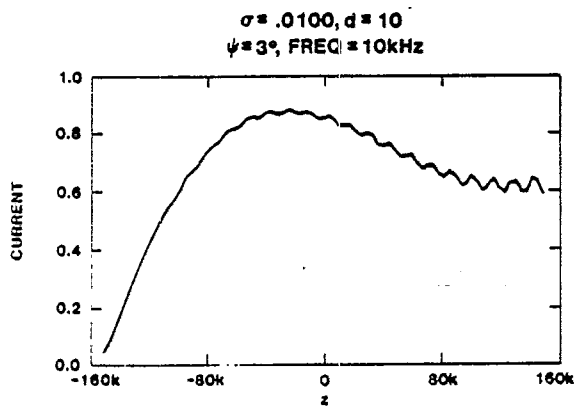


Figure 13. Induced Current (in Amps) Is Shown as the Vertical Axis and the Position on the Wire (in Meters) Is Shown as the Horizontal Axis. The current is calculated for a grazing angle denoted as ψ , matched load, and a frequency denoted as f .

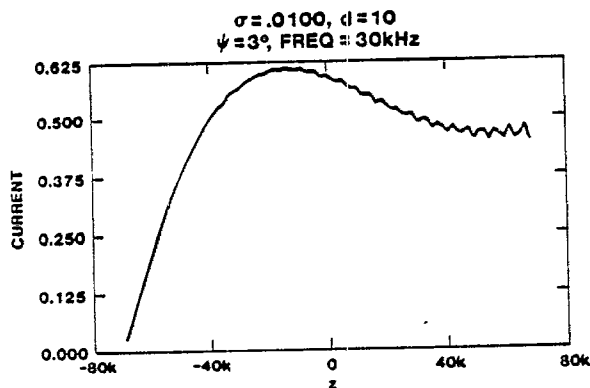


Figure 14. Induced Current (in Amps) Is Shown as the Vertical Axis and the Position on the Wire (in Meters) Is Shown as the Horizontal Axis. The current is calculated for a grazing angle denoted as ψ , matched load, and a frequency denoted as f .

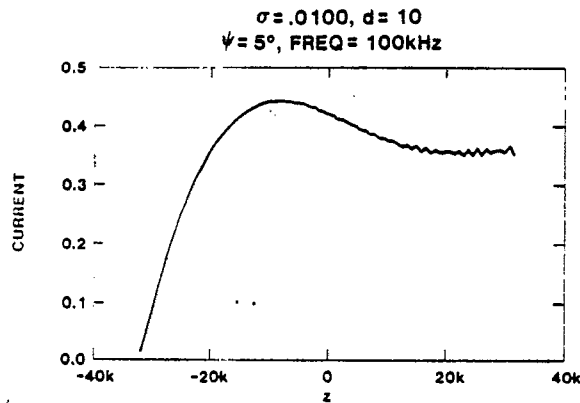


Figure 15. Induced Current (in Amps) Is Shown as the Vertical Axis and the Position on the Wire (in Meters) Is Shown as the Horizontal Axis. The current is calculated for a grazing angle denoted as ψ , matched load, and a frequency denoted as f .

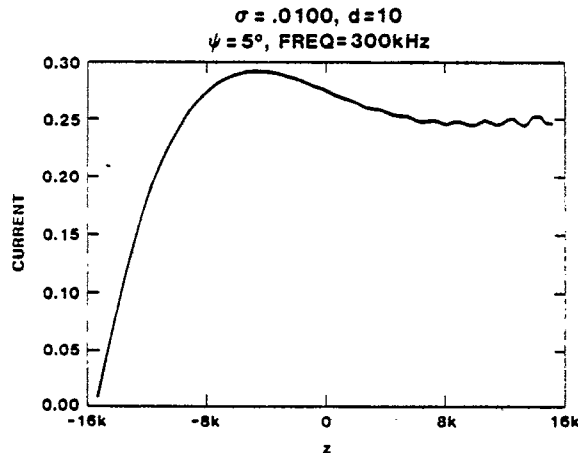


Figure 16. Induced Current (in Amps) Is Shown as the Vertical Axis and the Position on the Wire (in Meters) Is Shown as the Horizontal Axis. The current is calculated for a grazing angle denoted as ψ , matched load, and a frequency denoted as f .

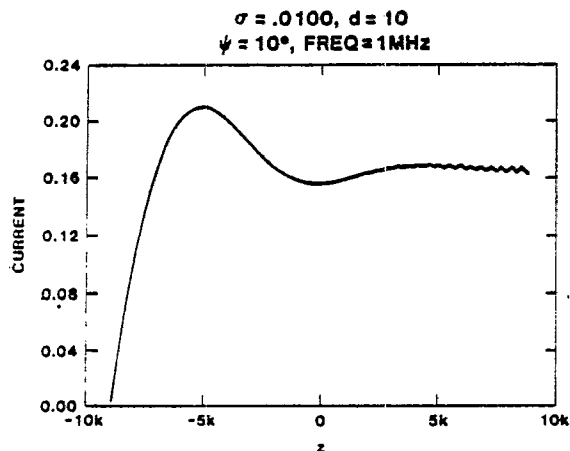


Figure 17. Induced Current (in Amps) Is Shown as the Vertical Axis and the Position on the Wire (in Meters) Is Shown as the Horizontal Axis. The current is calculated for a grazing angle denoted as ψ , matched load, and a frequency denoted as f .

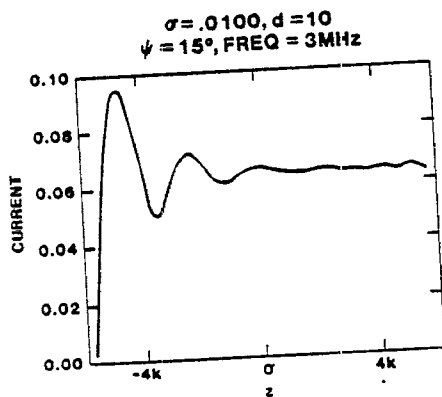


Figure 18. Induced Current (in Amps) Is Shown as the Vertical Axis and the Position on the Wire (in Meters) Is Shown as the Horizontal Axis. The current is calculated for a grazing angle denoted as ψ , matched load, and a frequency denoted as f .

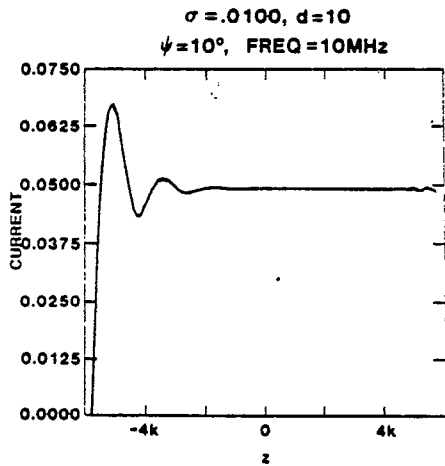


Figure 19. Induced Current (in Amps) Is Shown as the Vertical Axis and the Position on the Wire (in Meters) Is Shown as the Horizontal Axis. The current is calculated for a grazing angle denoted as ψ , matched load, and a frequency denoted as f .

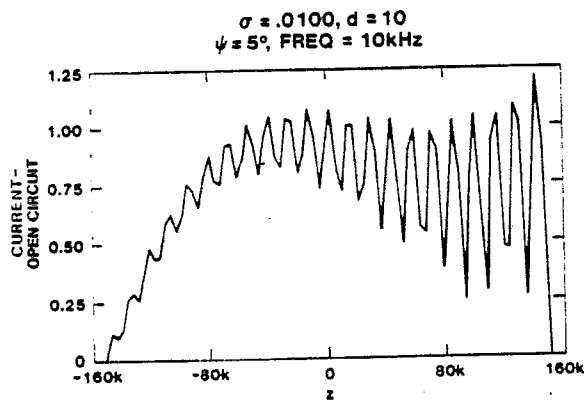


Figure 20. Induced Current (in Amps) Is Shown as the Vertical Axis and the Position on the Wire (in Meters) Is Shown as the Horizontal Axis. The current is calculated for a grazing angle denoted as ψ , a frequency denoted as f , and open-circuited at both ends.

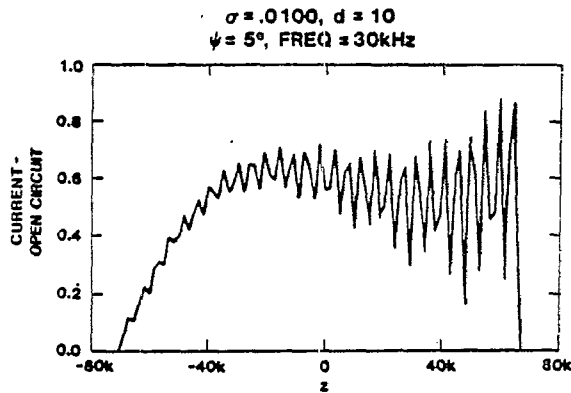


Figure 21. Induced Current (in Amps) Is Shown as the Vertical Axis and the Position on the Wire (in Meters) Is Shown as the Horizontal Axis. The current is calculated for a grazing angle denoted as ψ , a frequency denoted as f , and open-circuited at both ends.

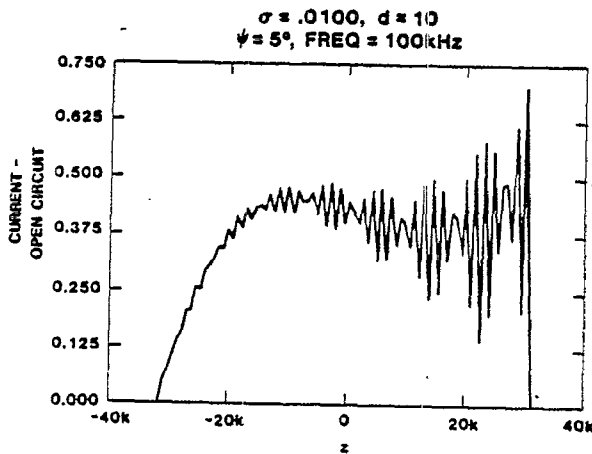


Figure 22. Induced Current (in Amps) Is Shown as the Vertical Axis and the Position on the Wire (in Meters) Is Shown as the Horizontal Axis. The current is calculated for a grazing angle denoted as ψ , a frequency denoted as f , and open-circuited at both ends.

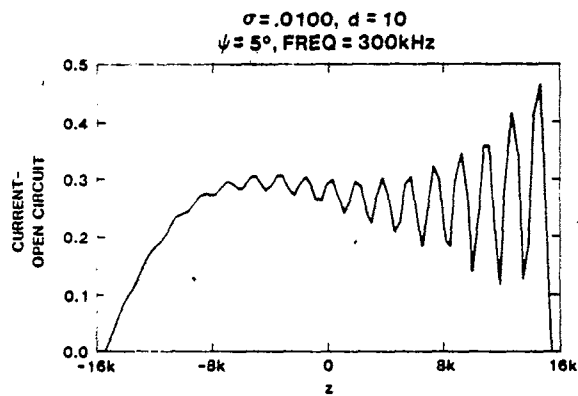


Figure 23. Induced Current (in Amps) Is Shown as the Vertical Axis and the Position on the Wire (in Meters) Is Shown as the Horizontal Axis. The current is calculated for a grazing angle denoted as ψ , a frequency denoted as f , and open-circuited at both ends.

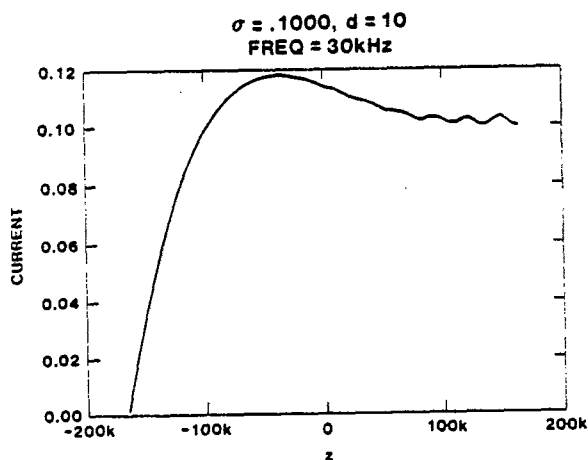


Figure 24. Induced Current (in Amps) Caused by a Lateral Wave Is Shown as the Vertical Axis and the Position on the Wire (in Meters) Is Shown as the Horizontal Axis. The current is calculated for a frequency denoted as f , and matched load at both ends.

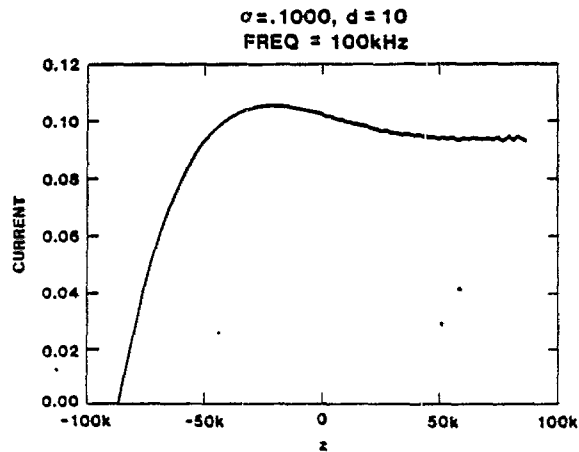


Figure 25. Induced Current (in Amps) Caused by a Lateral Wave Is Shown as the Vertical Axis and the Position on the Wire (in Meters) Is Shown as the Horizontal Axis. The current is calculated for a frequency denoted as f , and matched load at both ends.

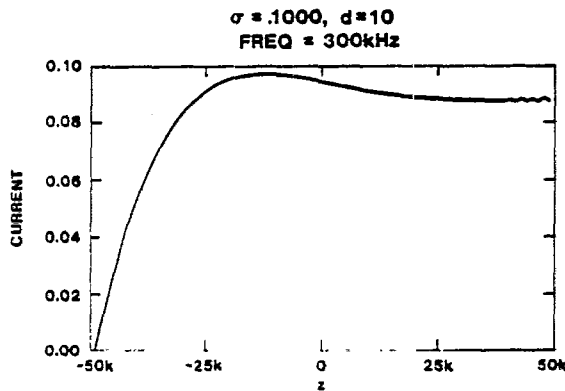


Figure 26. Induced Current (in Amps) Caused by a Lateral Wave Is Shown as the Vertical Axis and the Position on the Wire (in Meters) Is Shown as the Horizontal Axis. The current is calculated for a frequency denoted as f , and matched load at both ends.

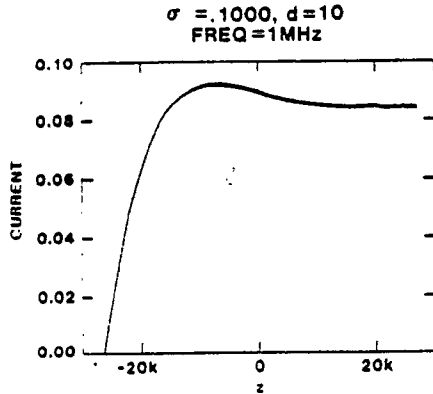


Figure 27. Induced Current (in Amps) Caused by a Lateral Wave Is Shown as the Vertical Axis and the Position on the Wire (in Meters) Is Shown as the Horizontal Axis. The current is calculated for a frequency denoted as f , and matched load at both ends.

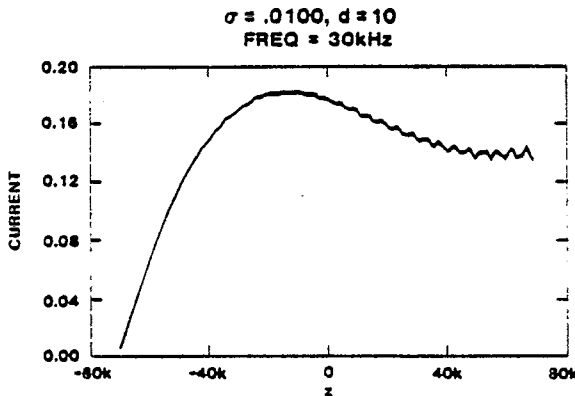


Figure 28. Induced Current (in Amps) Caused by a Lateral Wave Is Shown as the Vertical Axis and the Position on the Wire (in Meters) Is Shown as the Horizontal Axis. The current is calculated for a frequency denoted as f , and matched load at both ends.

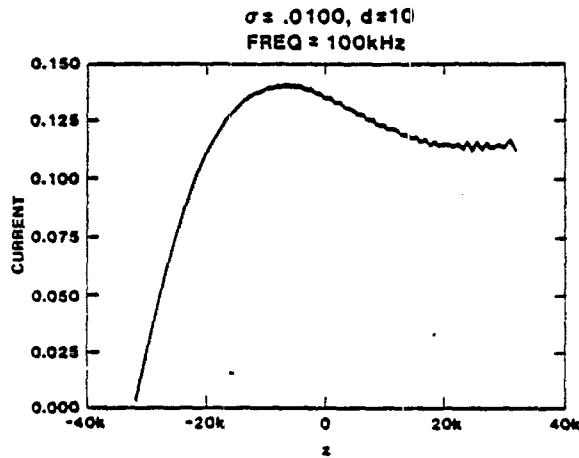


Figure 29. Induced Current (in Amps) Caused by a Lateral Wave Is Shown as the Vertical Axis and the Position on the Wire (in Meters) Is Shown as the Horizontal Axis. The current is calculated for a frequency denoted as f , and matched load at both ends.

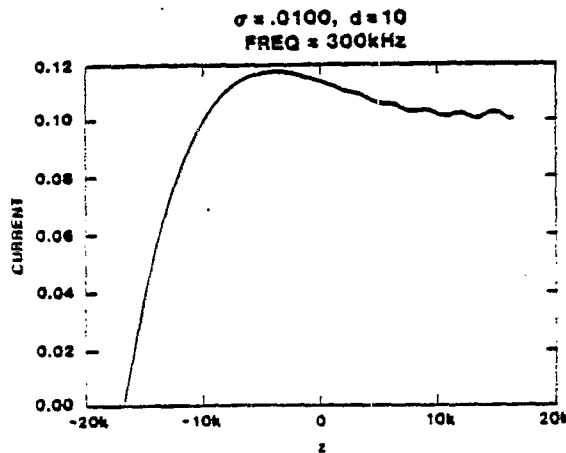


Figure 30. Induced Current (in Amps) Caused by a Lateral Wave Is Shown as the Vertical Axis and the Position on the Wire (in Meters) Is Shown as the Horizontal Axis. The current is calculated for a frequency denoted as f , and matched load at both ends.

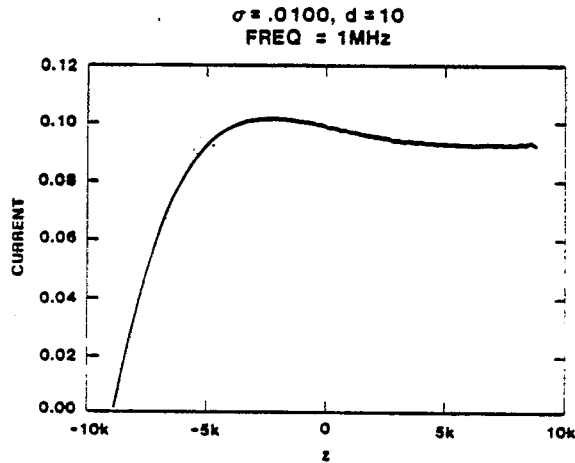


Figure 31. Induced Current (in Amps) Caused by a Lateral Wave Is Shown as the Vertical Axis and the Position on the Wire (in Meters) Is Shown as the Horizontal Axis. The current is calculated for a frequency denoted as f , and matched load at both ends.

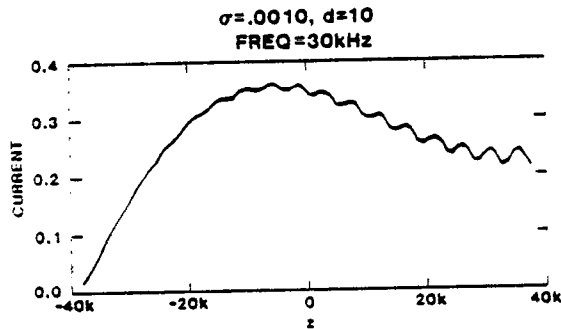


Figure 32. Induced Current (in Amps) Caused by a Lateral Wave Is Shown as the Vertical Axis and the Position on the Wire (in Meters) Is Shown as the Horizontal Axis. The current is calculated for a frequency denoted as f , and matched load at both ends.

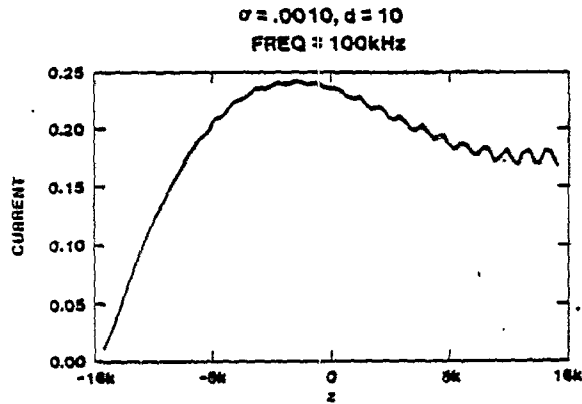


Figure 33. Induced Current (in Amps) Caused by a Lateral Wave Is Shown as the Vertical Axis and the Position on the Wire (in Meters) Is Shown as the Horizontal Axis. The current is calculated for a frequency denoted as f , and matched load at both ends.

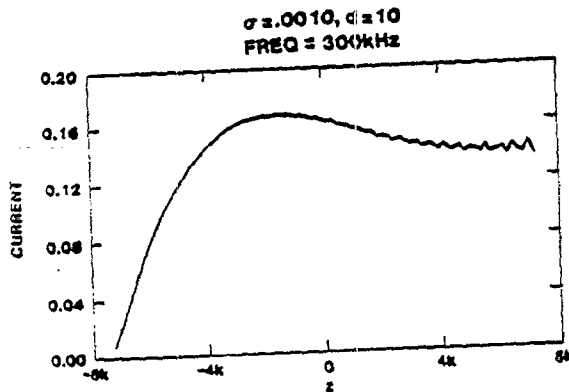


Figure 34. Induced Current (in Amps) Caused by a Lateral Wave Is Shown as the Vertical Axis and the Position on the Wire (in Meters) Is Shown as the Horizontal Axis. The current is calculated for a frequency denoted as f , and matched load at both ends.

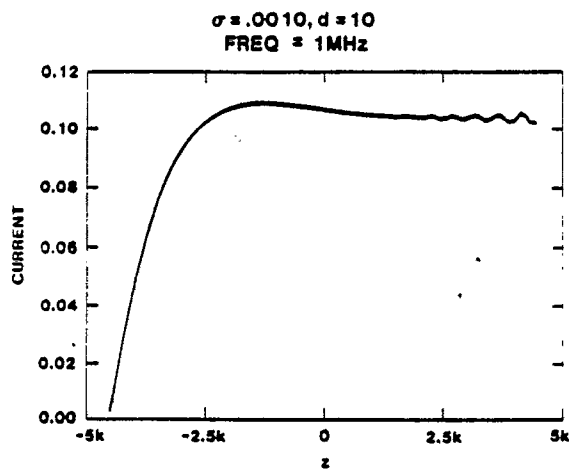


Figure 35. Induced Current (in Amps) Caused by a Lateral Wave Is Shown as the Vertical Axis and the Position on the Wire (in Meters) Is Shown as the Horizontal Axis. The current is calculated for a frequency denoted as f, and matched load at both ends.